J. Fluid Mech. (1993), *vol.* 248, *pp.* 449–475

Highly accelerated, free-surface flows

By MICHAEL S. LONGUET-HIGGINS
Institute for Nonlinear Science, University of California, San Diego, La Jolla, CA 92093-0402, USA

(Received 23 January 1992 and in revised form 29 September 1992)

Accelerations exceeding $20\,g$ in surface waves have been observed both in experiments and in numerically computed flows with a free surface. The present paper describes a family of analytic solutions which display such behaviour. They are expressible in parametric form as

$$z = F\sinh\omega + \mathrm{i}G\cosh\omega + \gamma\omega + \mathrm{i}H,$$

where F, G and H are functions of the time t only, and γ is linear in t. ω is a complex parameter which is real at the free surface. The functions $F(t)$ and $G(t)$ satisfy two nonlinear, coupled ODEs, which can be solved numerically. Typically the solutions pass through an 'inertial shock', or singularity in the time, where the displacements vary as $t^{\frac{2}{3}}$, the velocities as $t^{-\frac{1}{3}}$ and the accelerations as $t^{-\frac{4}{3}}$. In this class of solution the free surface develops a cusp as $t\to\infty$. In a special case, F and G vary as $t^{\frac{4}{7}}$ and the cusp is reached in finite time. Gravity is neglected, but plays a part in setting up the initial conditions for the highly accelerated flow.

In future papers it will be shown that more general solutions exist in which the acceleration is momentarily large but bounded.

1. Introduction

Some interesting examples of very high accelerations occurring in surface gravity waves were recently reported by Cooker & Peregrine (1990); see also Peregrine & Cooker (1991). Their numerical calculations of steep waves meeting a vertical wall (or of two such opposite waves meeting) show that the formation of a wave trough near the wall is sometimes followed surprisingly by a thin vertical jet which shoots upwards with accelerations typically of 20–50 g, and occasionally as great as 1000 g (Peregrine & Cooker 1991). The jet is accompanied by correspondingly large pressures and pressure gradients at the wall itself.

Upward-pointing jets induced by solitary waves meeting a wall have also been recorded experimentally by Nishimura & Takewaka (1990). Such jets are often seen against the bow of a ship. It is likely that the axial jets seen in standing waves and collapsing bubbles (Longuet-Higgins 1983*c*) are closely related.

In spite of these calculations and observations, there is little understanding of the phenomenon, or of the range of conditions under which it occurs. For this purpose, purely numerical calculations are inadequate, and cannot always describe accurately the asymptotic form of the fluid flow when the free surface develops a sharp curvature. What is required is an analytic solution which can unify the different numerical computations and define the asymptotic behaviour of the flow.

Exact solutions for time-dependent flows with a free surface are rare. A flow which has some of the appropriate features is the 'Dirichlet hyperbola'; see Longuet-Higgins (1972). In this flow the free surface has the form of hyperbola with varying

angle θ between the asymptotes. When θ approaches 90°, the velocity and acceleration become infinite, like $t^{-\frac{1}{3}}$ and $t^{-\frac{4}{3}}$ respectively, where t is the time measured from the critical instant. A physical explanation has been given by Longuet-Higgins (1983*c*). There are two weaknesses in this solution, however. One is the very restricted form of the free surface, which does not allow the formation of a cusp – only a thin, ultimately parabolic, jet as $t \to \infty$. Secondly, it is not immediately clear how the solution is to pass through the infinity at time $t = 0$.

These considerations prompted the author to search for a more general analytic solution. In this and two companion papers use is made of a parametric representation of irrotational flow first suggested by John (1953). The representation is sometimes called 'semi-Lagrangian'. The present author has already expressed the Dirichlet hyperbola and its extension to a rotating free surface, in a semi-Lagrangian form; see Longuet-Higgins (1983*a*, *b*). With this representation, as is shown in the present paper, it is a simple matter to generalize the Dirichlet hyperbola by adding an extra term linear in ω and t. This has a non-trivial effect; for example it makes possible the formation of a cusp at the free surface. It also gives rise to a beautiful family of solutions which have the principally desired feature, the occurrence of an inertial shock at a certain instant. It can be shown, moreover, that by the addition of two further terms the infinite pressure and acceleration are replaced by momentarily large but finite values (see §13 below).

The plan of the present paper is as follows. Since it may be convenient for many readers, a brief introduction to the semi-Lagrangian representation is given in §2. In the following section we give the expression for the Dirichlet hyperbola in semi-Lagrangian form, and in §4 state the first generalization. It is shown that this leads to two coupled, nonlinear, ordinary differential equations for the coefficients $F(t)$ and $G(t)$ as functions of the time. One of these equations (equation (4.10)) follows from the free-surface condition, the other, (4.11), from the condition that the flow be free of singularities within the fluid. In §5 we see that in the simplest case, (4.10) leads to a simple mapping of the trajectories in the (F, G)-plane. The time-dependence of the solutions is described in §6, including the mapping of the 'shock line'. In §7 we describe the behaviour of the solutions in the neighbourhood of the shock line, and show that F and G behave like $t^{\frac{2}{3}}$ there, just as for the Dirichlet hyperbola. There is one exceptional trajectory (§10) where the time-dependence is like $t^{\frac{4}{7}}$. Knowing this behaviour one can integrate up to and across the shock line without difficulty (§8). The mapping of the solutions in the general case is described in §§11 and 12. Section 13 contains some discussion and an indication of further developments.

2. Parametric representation

The basis of the following analysis is the semi-Lagrangian method of representing any time-dependent, irrotational, free-surface flow in two dimensions (x, y). In this representation, both the complex coordinate $z = x + \mathrm{i}y$ and the complex velocity potential $\chi = \phi + \mathrm{i}\psi$ are given in terms of a complex parameter ω, and the time t. Thus we let

$$z = z(\omega, t), \quad \chi = \chi(\omega, t), \tag{2.1}$$

where z and χ are analytic functions of ω. On the free surface, where the pressure is constant, it is supposed (i) that ω is real and (ii) that ω is a Lagrangian coordinate, that is ω is constant following a particle. Hence the velocity vector (u, v) is given by

$$u + \mathrm{i}v = z_t(\omega, t), \quad \omega \text{ real}, \tag{2.2}$$

a subscript denoting partial differentiation. Moreover, the particle acceleration at the surface is $z_{tt}(\omega, t)$, and since the pressure gradient has to be normal to the free surface it follows from the equations of motion that the acceleration vector z_{tt} is normal to the free surface, gravity being neglected, or in the frame of reference in free-fall. But the tangent to the free surface is in the direction of $z_\omega(\omega, t)$. Hence the free-surface condition may be written

$$z_{tt} = \mathrm{i}Rz_\omega, \tag{2.3}$$

where $R(\omega, t)$ is some function of ω and t which is *real* at the free surface.

In the interior of the fluid where ω is not real, (2.2) does not apply, but rather

$$u + \mathrm{i}v = z_t(\omega^*, t) \tag{2.4}$$

where an asterisk denotes the complex conjugate. The reason for this requirement is immediately clear, for then we have

$$\mathrm{d}\chi/\mathrm{d}z = u - \mathrm{i}v = z_t^*(\omega, t), \tag{2.5}$$

where z^* denotes the complex conjugate function to z. Hence

$$\frac{\mathrm{d}\chi}{\mathrm{d}\omega} = \frac{\mathrm{d}\chi}{\mathrm{d}z}\frac{\mathrm{d}z}{\mathrm{d}\omega} = z_t^*(\omega, t)\, z_\omega(\omega, t). \tag{2.6}$$

Both sides being now functions of ω and not involving ω^*, we may integrate with respect to ω to obtain in general

$$\chi = \int z_t^*(\omega, t)\, z_\omega(\omega, t)\, \mathrm{d}\omega. \tag{2.7}$$

An important subsidiary condition is the following. Generally, the coordinate transformation represented by $z(\omega, t)$ is regular, z being an analytic function of ω and t. However, there will usually be singularities, the simplest of which occurs when $z_\omega = 0$, say when $z = z_0$. In the neighbourhood of such a point

$$(z - z_0) = (\omega - \omega_0)\, z_\omega + \tfrac{1}{2}(\omega - \omega_0)^2 z_{\omega\omega} + \ldots. \tag{2.8}$$

Since z_ω vanishes, we see that

$$(\omega - \omega_0) \propto (z - z_0)^{\frac{1}{2}} \tag{2.9}$$

so that the velocity field $(u - \mathrm{i}v)$, represented by $z_t^*(\omega, t)$ has a branch point unless $z_t^*(\omega, t)$ also has a similar singularity, that is to say

$$z_{t\omega}^* = 0 \quad \text{when} \quad \omega = \omega_0. \tag{2.10}$$

The condition (2.10), which is applied at one or more points *inside* the fluid, will be seen to play a vital role in the following solutions.

3. The Dirichlet hyperbola

One interesting solution to the equations in §2 is given by

$$z = F \sinh \omega + \mathrm{i}G \cosh \omega \tag{3.1}$$

(see Longuet-Higgins 1983*a*, *b*), F and G being real functions of the time only. For then

$$z_{tt} = F'' \sinh \omega + \mathrm{i}G'' \cosh \omega, \tag{3.2}$$

where a prime denotes $\mathrm{d}/\mathrm{d}t$, while

$$z_\omega = F\cosh\omega + \mathrm{i}G\sinh\omega. \tag{3.3}$$

Hence the boundary condition (2.3) is satisfied provided that

$$F'' = -RG, \qquad G'' = RF. \tag{3.4}$$

On eliminating R from these equations we have

$$FF'' + GG'' = 0. \tag{3.5}$$

As for the interior condition, it is clear from (3.3) that z_ω will vanish on the axis of symmetry (ω pure imaginary) when

$$\sinh\omega = \frac{\pm\mathrm{i}F}{(F^2+G^2)^{\frac{1}{2}}}, \quad \cosh\omega = \frac{\pm G}{(F^2+G^2)^{\frac{1}{2}}} \tag{3.6}$$

and so

$$z = \pm\mathrm{i}(F^2+G^2)^{\frac{1}{2}}. \tag{3.7}$$

However, we have also from (3.3) that

$$z^*_{\omega t} = F'\cosh\omega - \mathrm{i}G'\sinh\omega. \tag{3.8}$$

The zeros of $z^*_{\omega t}$ therefore coincide with those of z_ω provided that

$$F'/F = -G'/G, \tag{3.9}$$

that is

$$F'G + FG' = 0 \tag{3.10}$$

or

$$FG = \text{constant}. \tag{3.11}$$

From the two equations (3.4) and (3.11) a differential equation for $R(t)$ and hence F and G can be obtained (see Longuet-Higgins 1983*b*). An alternative method is given in Appendix A.

The free surface corresponding to (3.1) is clearly a hyperbola:

$$\frac{x^2}{F^2} - \frac{y^2}{G^2} + 1 = 0 \tag{3.12}$$

with semi-axes equal to F and G respectively. The branch points (3.7) are at the two foci, and *both* are annulled by the condition (3.11).

We remark that since the fluid is on one side only of the free surface, it is really unnecessarily to annul both of the branch points; only the branch point within the fluid itself need be annulled. Hence we suspect the existence of a more general analytic expression of this type in which only one branch point is annulled.

4. A first generalization

The key to a more general type of solution than that of §3 is to add to the right-hand side of (3.1) a term linear in both ω and t. Thus let

$$z = F\sinh\omega + \mathrm{i}G\cosh\omega + \gamma\omega + \mathrm{i}H, \tag{4.1}$$

where

$$\gamma = \alpha + \beta t, \tag{4.2}$$

α and β being real constants, and H a function of the time only, to be determined. Then we have

$$z_{tt} = F''\sinh\omega + \mathrm{i}G''\cosh\omega + \mathrm{i}H'' \tag{4.3}$$

and

$$z_{\omega} = F\cosh\omega + \mathrm{i}G\sinh\omega + \gamma. \tag{4.4}$$

Equation (2.3) is therefore satisfied provided that

$$F'' = -RG, \qquad G'' = RF \tag{4.5}$$

as before, and further

$$H'' = R(\alpha + \beta t). \tag{4.6}$$

Clearly H'' represents an additional upward acceleration of the fluid as a whole.

To free the flow of branch points, any zeros of z_{ω} (equation (4.4)) that lie in the fluid must be annulled by a zero of

$$z^*_{\omega t} = F'\cosh\omega - \mathrm{i}G'\sinh\omega + \beta, \tag{4.7}$$

since $\beta = \gamma'$ by (4.2). Thus we have two equations in e^{ω}:

$$\left.\begin{aligned} 2z_{\omega} &= (F+\mathrm{i}G)\,\mathrm{e}^{\omega} + 2\gamma + (F-\mathrm{i}G)\,\mathrm{e}^{-\omega} = 0, \\ 2z^*_{\omega t} &= (F'-\mathrm{i}G')\,\mathrm{e}^{\omega} + 2\beta + (F'+\mathrm{i}G')\,\mathrm{e}^{-\omega} = 0, \end{aligned}\right\} \tag{4.8}$$

which must share at least one common root. The condition for this is the vanishing of the discriminant of the two equations, that is

$$\begin{vmatrix} (F+\mathrm{i}G) & 2\gamma & (F-\mathrm{i}G) & 0 \\ (F'-\mathrm{i}G') & 2\beta & (F'+\mathrm{i}G') & 0 \\ 0 & (F+\mathrm{i}G) & 2\gamma & (F-\mathrm{i}G) \\ 0 & (F'-\mathrm{i}G') & 2\beta & (F'+\mathrm{i}G') \end{vmatrix} = 0. \tag{4.9}$$

(Equation (4.9) may be derived by multiplying each of (4.8) by e^{ω} and then eliminating $\mathrm{e}^{2\omega}$, e^{ω}, 1 and $\mathrm{e}^{-\omega}$ from all four equations.)

Though apparently possessing both real and imaginary parts, the determinant can be seen to be purely real. For, if we interchange the third and fourth rows, the resulting determinant has rotational symmetry about its central point except that i is replaced by $-\mathrm{i}$. The determinant thus equals its complex conjugate, and so is real.

On expansion we find

$$\Phi \equiv (F'G + FG')^2 - (\beta F - \gamma F')^2 - (\beta G + \gamma G')^2 = 0. \tag{4.10}$$

This is a nonlinear, ordinary differential equation relating F and G. In addition, we have the second-order equation

$$FF'' + GG'' = 0 \tag{4.11}$$

as before, obtained by eliminating R from (4.5). If F and G can be determined from (4.10) and (4.11) we can then find R from either of equations (4.5). Then H is found by integrating (4.6) twice with respect to t.

The branch points of the representation $z(\omega, t)$ correspond to the two zeros of z_{ω}, see (4.8). These are

$$\mathrm{e}^{\omega} = [-\gamma \pm \mathrm{i}(F^2 + G^2 - \gamma^2)^{\frac{1}{2}}]/(F + \mathrm{i}G). \tag{4.12}$$

Since $|\mathrm{e}^{\omega}| = 1$, ω is pure imaginary. Hence z, given by (4.1) reduces to

$$z = \pm\mathrm{i}(F^2 + G^2 - \gamma^2)^{\frac{1}{2}} + \gamma\omega + \mathrm{i}H. \tag{4.13}$$

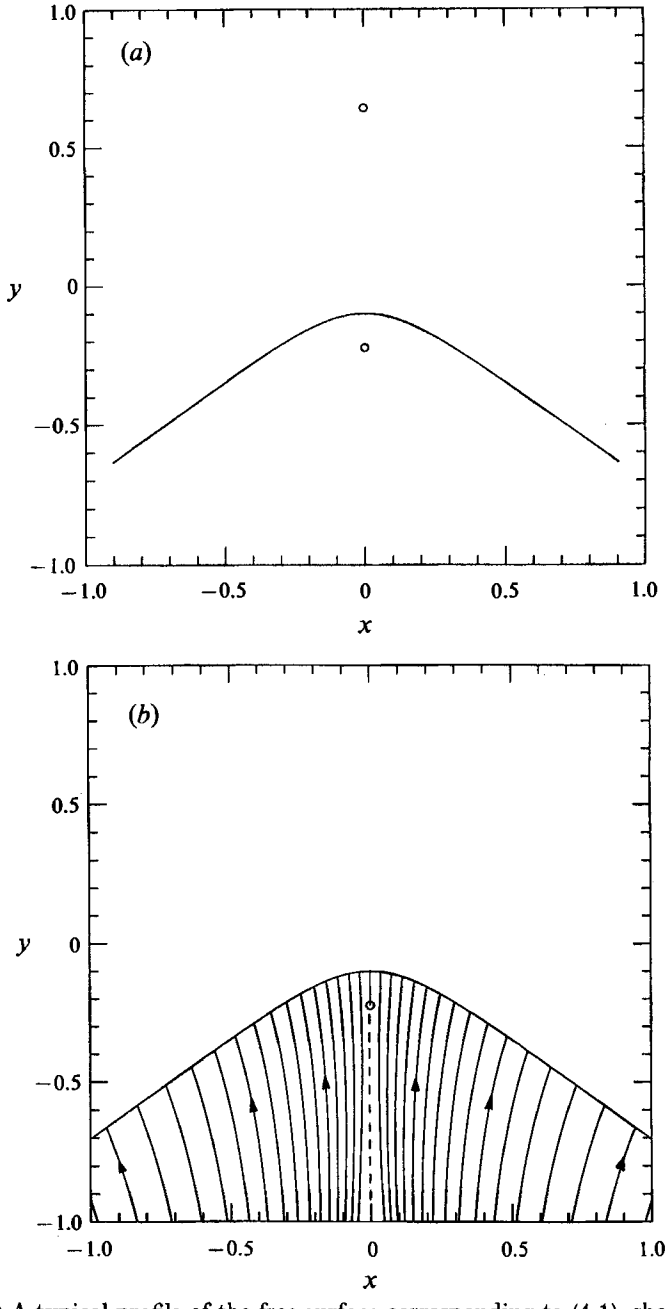

FIGURE 1. (*a*) A typical profile of the free surface corresponding to (4.1), showing the two branch points corresponding to zeros of z_ω. ($F = -1.5, G = -0.8$.) (*b*) Streamlines corresponding to the solution of (*a*) when (2.10) is satisfied at the lower branch point. ($F' = 1.0, G' = -2.0598$.)

Provided $(F^2+G^2-\gamma^2) > 0$, z also is pure imaginary, and the branch points lie on the imaginary axis (see figure 1*a*). This axis intersects the surface at $\omega = 0$, $z = \mathrm{i}(G+H)$. Thus provided $(F^2-\gamma^2) > 0$ one of the branch points always lies 'above' the free surface, and one 'below' the surface, so it is the negative branch point that is to be excluded.

From (4.1) it will be seen that when $(F+\gamma)=0$, then for small values of the parameter ω we have

$$x = \tfrac{1}{6}F\omega^3, \qquad y = G(1+\tfrac{1}{2}\omega^2)+H, \tag{4.14}$$

so the free surface (ω real) develops a cusp. Generally, for small ω, we have $x_\omega = F+\gamma$ whereas for large ω, x_ω will have the same sign as F. Hence the range $-\gamma < F < 0$ must be excluded since the free surface would then have a loop.

5. Map of the solutions: $\beta = 0$

To fix the ideas, let us take first the simplest case: $\beta = 0$. Equation (4.10) then reduces to

$$\Phi \equiv (F'G+FG')^2-\alpha^2(F'^2+G'^2) = 0, \tag{5.1}$$

that is

$$(G^2-\alpha^2)F'^2+2FGF'G'+(F^2-\alpha^2)G'^2 = 0. \tag{5.2}$$

For any given values of F and G this defines in general two directions in the (F,G)-plane given by

$$\frac{F'}{G'} = \frac{-FG\pm\alpha(F^2+G^2-\alpha^2)^{\frac{1}{2}}}{G^2-\alpha^2} \tag{5.3}$$

provided that

$$F^2+G^2-\alpha^2 \geqslant 0. \tag{5.4}$$

Assuming α to be positive, the set of directions corresponding to the positive sign in (5.3) is shown in figure 2. The circular region in the centre is excluded by (5.4). The pattern clearly has a 4-fold rotational symmetry about the origin.

The set of directions corresponding to the negative sign in (5.3) is exactly similar to figure 2, but with the opposite direction of rotation; the two patterns are mirror images of each other.

Equation (5.2) or its solution (5.3) is in fact the condition that at least one of the zeros of z_ω be annulled by one of the zeros of $z^*_{\omega t}$. Now the zeros of $z^*_{\omega t}$ are given, as in (4.12), by

$$e^\omega = [-\beta\pm i(F'^2+G'^2-\beta^2)^{\frac{1}{2}}]/(F'-iG') \tag{5.5}$$

and when $\beta = 0$ it is evident that the two roots cannot both annul roots of (4.12) (in which $\gamma = \alpha$) except in the special case $\alpha = 0$. Thus in general, only one root of the roots of $z_\omega = 0$ is annulled. It turns out that choosing the plus sign in (5.3) always annuls the singularity below the free surface (see figure 1) while choosing the minus sign annuls the singularity above the free surface. We shall be concerned only with the former case, for which the pattern of directions is as in figure 2.

It should be noted that while the subsidiary condition (2.10) is satisfied exactly at all times, this removes only the principal part of the singularity at $z_\omega = 0$. In figure 1(*b*) we have plotted the instantaneous streamlines for a solution in which the free surface is as in figure 1(*a*). This shows that on the part of the axis of symmetry below the branch point the streamlines are very nearly, but not quite, parallel to the axis. To accommodate the flow, we must assume a weak line sink along the y-axis between the branch point and $y = -\infty$. Thus, while the solution is not exact in this respect, it appears as a very good approximation.

We are interested especially in flows that develop upward-pointing cusps, without loops. This implies that, over some part of the trajectory, $F < -\alpha$ and $G < 0$. Clearly the trajectories of interest are confined to the region $-\infty < F < -\alpha$, $-\infty < G < \alpha$ shown in figure 3.

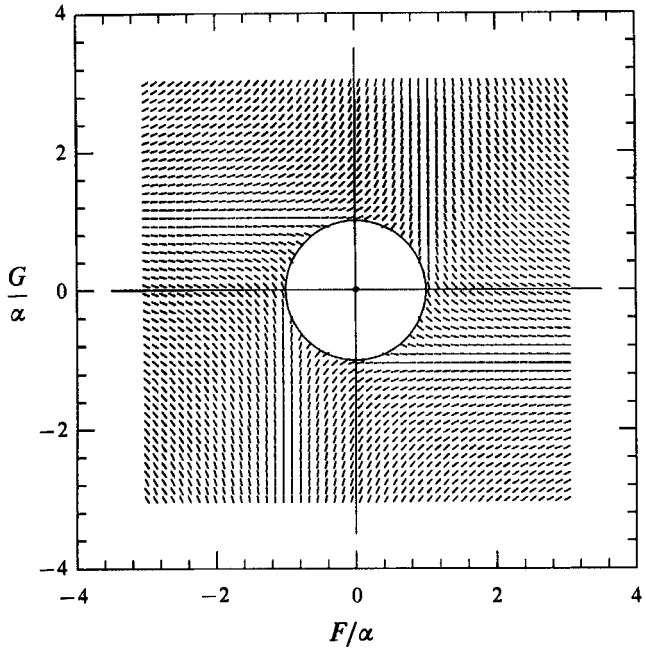

FIGURE 2. Directions of the trajectories of the coefficients F and G in the (F, G)-plane.

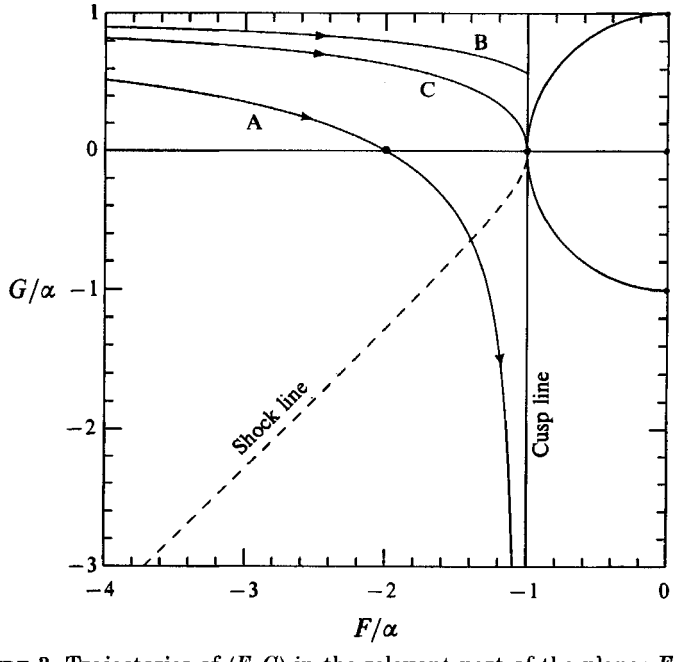

FIGURE 3. Trajectories of (F, G) in the relevant part of the plane: $F \leqslant -\alpha, G \leqslant 1$.

The trajectories are of three types. Type A starts from $F = -\infty$, $G \sim \alpha$ and becomes asymptotic to the cusp line $F = -\alpha$, $G < 0$. Each trajectory crosses the G-axis at some point $(F_0, 0)$ between $-\infty$ and $-\alpha$.

Type B also starts from $F = -\infty$, $G \sim \alpha$, but crosses the cusp line $F = -\alpha$ at some point where $G > 0$.

Type C, the 'critical trajectory', is intermediate between Types A and B. It touches the cusp line $F = -\alpha$ at $G = 0$. The section of the line $F = 0$, $G < 0$ should also be considered as part of this trajectory.

6. Time-dependence of the solutions

To solve the two coupled equations (4.11) and (5.1) for $F(t)$ and $G(t)$ we may first differentiate (5.1) with respect to the time to obtain

$$AF'' + BG'' + C = 0, \tag{6.1}$$

where

$$A = (F'G + FG')G - \alpha^2 F', \quad B = (F'G + FG')F - \alpha^2 G', \quad C = (F'G + FG')2F'G'. \tag{6.2}$$

Substituting for F'' and G'' from (4.5) we find

$$R = C/\Delta \tag{6.3}$$

where

$$\Delta = (AG - BF) = (F'G + FG')(G^2 - F^2) - \alpha^2(F'G - FG'). \tag{6.4}$$

Then F'', G'' and H'' are found from (4.5) and (4.6). Choosing initial values of F, G, F' and G' to satisfy (5.1) at a given time $t = t_0$ we can then integrate forwards (or backwards) to determine these quantities as functions of t.

As one would anticipate from the case $\alpha = 0$, the solution develops a singularity at a finite time $t = t_c$ at which time Δ vanishes and R becomes infinite. An explanation can be given as follows. If we think of (F, G) as coordinates of a particle in the (F, G)-plane, then (F'', G'') is the vector acceleration of the particle. Equation (4.11) then states that the radial component of the acceleration vanishes. Thus the particle moves as a small heavy steel ball in a thin, frictionless tube which is constrained to rotate about the origin $(0, 0)$.

Suppose the particle moves on a curved trajectory. If the curvature and the velocity are both non-vanishing, the particle has a non-zero acceleration normal to the trajectory. A crisis must therefore occur when the normal to the trajectory passes through the origin, that is when

$$FF' + GG' = 0. \tag{6.5}$$

As confirmation, note that by (5.1)

$$\alpha^2 = (FG' + F'G)^2/(F'^2 + G'^2). \tag{6.6}$$

Hence on substitution in (6.4) we find, after some simplification,

$$\Delta = (FG' + F'G)(F^2F'^2 - G^2G'^2)/(F'^2 + G'^2). \tag{6.7}$$

So by (6.2) and (6.3)

$$R = \frac{2F'G'(F'^2 + G'^2)}{(FF' + GG')(FF' - GG')}. \tag{6.8}$$

Clearly R becomes infinite when $(FF' + GG') = 0$ and if $F'G'$ is not zero, in accordance with (6.5).

To interpret the second factor in the denominator, note that on the critical circle

$$F^2 + G^2 = \alpha^2 \tag{6.9}$$

we have, again by (5.1) or (6.6),

$$(FF' - GG')^2 = 0. \tag{6.10}$$

Thus the critical circle is also part of the locus $\Delta = 0$ or of $R = \infty$. However, it lies outside the region of interest for us.

Lastly we note that a general expression for the curvature κ of the trajectory is

$$\kappa = \frac{F'G'' - F''G'}{(F'^2 + G'^2)^{\frac{3}{2}}}. \tag{6.11}$$

So on substitution for F'' and G'' from (4.5),

$$\kappa = \frac{FF' + GG'}{(F'^2 + G'^2)^{\frac{5}{2}}} R. \tag{6.12}$$

Hence

$$R = \frac{\kappa q^3}{FF' + GG'}, \tag{6.13}$$

where q is the 'velocity' $(F'^2 + G'^2)^{\frac{1}{2}}$. Hence if neither κ nor q vanishes, R must become infinite when (6.5) is satisfied.

A physical interpretation of the singularity in terms of the fluid flow was previously given by Longuet-Higgins (1983*c*) in the special case $\alpha = 0$. Essentially what occurs is an *inertial shock* necessitated by the kinematics of the flow field, combined with the local form of the free surface. For this reason it is appropriate to call the locus $(FF' + GG') = 0$ the 'shock line'. It is of course a line drawn in the (F, G)-plane, not in physical space.

In the next section we investigate the behaviour of $F(t)$ and $G(t)$ in the neighbourhood of the shock line.

7. Neighbourhood of the shock line

In the neighbourhood of the shock line let us write

$$F = F_c + \xi, \quad G = G_c + \eta \tag{7.1}$$

where the suffix c denotes values on the shock-line itself, and (ξ, η) are of order $\epsilon\alpha$, say, where $\epsilon \ll 1$. Substituting in (5.1) we have then

$$\Phi \equiv [(G_c + \eta)^2 - \alpha^2]\,\xi'^2 + 2(F_c + \xi)(G_c + \eta)\,\xi'\eta' + [(F_c + \xi)^2 - \alpha^2]\,\eta'^2 = 0. \tag{7.2}$$

Solving for ξ'/η' as before, and retaining terms of order ϵ^0 and ϵ^1 only we find

$$\xi'/\eta' = a + b\xi + c\eta, \tag{7.3}$$

where

$$a = \frac{\alpha D - FG}{G^2 - \alpha^2}, \quad b = \frac{\alpha F - GD}{(G^2 - \alpha^2)\,D}, \quad c = \frac{\alpha G - FD}{(G^2 - \alpha^2)\,D} + \frac{2G(FG - \alpha D)}{(G^2 - \alpha^2)^2} \tag{7.4}$$

and we have written $D = (F^2 + G^2 - \alpha^2)^{\frac{1}{2}}$, suppressing the suffices. After some reduction we find that

$$c = ab. \tag{7.5}$$

Suppose now that on the trajectory ξ is expanded in a Taylor series in η:

$$\xi = a\eta + \tfrac{1}{2}\lambda\eta^2 + \ldots, \tag{7.6}$$

where λ is a constant to be determined. This implies that

$$\xi'/\eta' = \mathrm{d}\xi/\mathrm{d}\eta = a + \lambda\eta. \tag{7.7}$$

But from (7.3) we have, to order ϵ,

$$\xi'/\eta' = a+(ab+c)\,\eta. \tag{7.8}$$

Therefore
$$\lambda = ab+c = 2ab \tag{7.9}$$

by (7.5). Altogether then we have

$$\xi = a\eta+ab\eta^2 \tag{7.10}$$

on the trajectory.

On the other hand from (4.11) we have

$$(F_c+\xi)\,\xi''+(G_c+\eta) = 0. \tag{7.11}$$

But from (7.6)
$$\xi'' = (a+\lambda\eta)\,\eta''+\lambda\eta'^2. \tag{7.12}$$

Substituting for ξ'' in (7.7) and noting that the lowest-order terms must vanish, i.e.

$$aF_c+G_c = 0, \tag{7.13}$$

we obtain correct to order ϵ^2 the equation

$$(a^2+\lambda F_c+1)\,\eta\eta''+\lambda F_c\,\eta'^2 = 0 \tag{7.14}$$

for $\eta(t)$. The only solution that vanishes as $t\to t_c$ is

$$\eta = \nu(t-t_c)^n \tag{7.15}$$

where
$$n = \frac{a^2+\lambda F_c+1}{a^2+2\lambda F_c+1} = \frac{a^2+2abF_c+1}{a^2+4abF_c+1}. \tag{7.16}$$

Now from the expressions for a and b given in (7.4) it is straightforward to establish the identity

$$a^2+1 = 2abF. \tag{7.17}$$

From (7.16) it then follows that

$$n = \tfrac{2}{3}. \tag{7.18}$$

Thus we have shown that, in the neighbourhood of the shock line, F and G tend to finite values F_c and G_c, but that velocities, like F' and G', become infinite $(t-t_c)^{-\frac{1}{3}}$; the accelerations and the pressure behave like $(t-t_c)^{-\frac{4}{3}}$. This generalizes the results previously obtained in the case $\alpha = 0$ (Longuet-Higgins 1972).

8. Integrating through the shock line

As a consequence of the analysis in §7, we now have a method of continuing the integration of F and G through the singularity. For, when sufficiently close to the shock line we have from (6.2) and (6.3), since $F', G' \propto t^{-\frac{1}{3}}$,

$$C \sim (t-t_c)^{-1}, \quad R \sim (t-t_c)^{-\frac{4}{3}}. \tag{8.1}$$

Hence
$$\Delta = C/R \sim (t-t_c)^{\frac{1}{3}}. \tag{8.2}$$

Thus Δ^3 behaves linearly with t, so by linear extrapolation of Δ^3 in the neighbourhood of $\Delta = 0$ we can determine accurately the critical instant t_c.

Then, if $F(t)$ and $G(t)$ are integrated up to a time t_1, say, close to t_c, we can find the value F_c of F at the critical time by linear extrapolation of F with respect to $(t-t_c)^{\frac{2}{3}}$. Having found F_c and likewise G_c we can cross over to the time

$$t_2 = 2t_c-t_1 \tag{8.3}$$

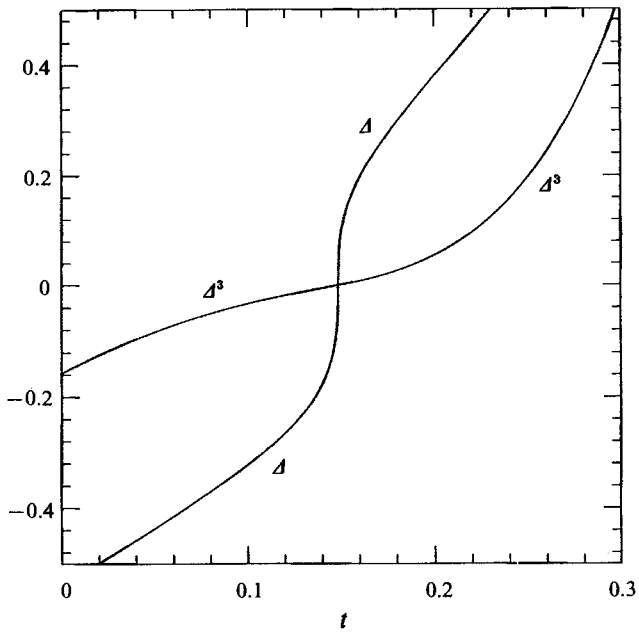

FIGURE 4. The behaviour of Δ and Δ^3 in the neighbourhood of $t = t_c$ for the typical trajectory $(F_0, G_0) = (-1.3, 0)$, $F'_0 = 1.0$.

on the far side of the singularity by taking

$$F(t_2) = 2F(t_c) - F(t_1), \qquad F'_2(t_2) = F'_2(t_1), \tag{8.4}$$

and similarly for $G(t_2)$ and $G'(t_2)$. Step-by-step integration can then start again from $t = t_2$.

Figure 4 shows the result of this procedure for a typical trajectory of Type A, when $F_0 = -1.30$ and $F'_0 = 1.0$. Both Δ and Δ^3 are plotted as functions of t. It will be seen that the graph of Δ *vs.* t is that of a typical cubic curve, and that Δ^3 behaves smoothly and linearly versus the time.

The corresponding velocity $$y_t = G' + H' \tag{8.5}$$

and acceleration $$y_{tt} = G'' + H'' \tag{8.6}$$

of the surface particle $\omega = 0$ are shown in figure 5. In the limit as $t \to t_c$, y_{tt} is symmetric about $t = t_c$, and y_{tt} is antisymmetric. The pressure gradient p_y is similar to y_{tt}.

As a practical point we mention that sufficiently close to $t = t_c$ it is convenient to take time increments $\mathrm{d}t$ corresponding to equal increments of the function $f = \ln \Delta$. Since $(t - t_c) \propto \Delta^3$ this implies that

$$\mathrm{d}t \propto 3|t - t_c|\,\mathrm{d}f \propto |t - t_c|. \tag{8.7}$$

The time steps in the integration were reduced until the results converged sufficiently accurately. Typically, as in figures 4–6, $\mathrm{d}t$ was taken as 0.5×10^{-4}. In the neighbourhood of the shock line, defined by $|\Delta| < 0.005$, $\mathrm{d}t$ was chosen to correspond to increments 0.005 in $\ln \Delta$. The limiting t_1 was chosen to be the first instant at which $|\Delta| < 10^{-6}$. On the far side of the shock line ($t > t_2$) the procedure was reversed. Note that since t_c and t_2 were not round numbers, neither were the chosen times t, for $t > t_1$.

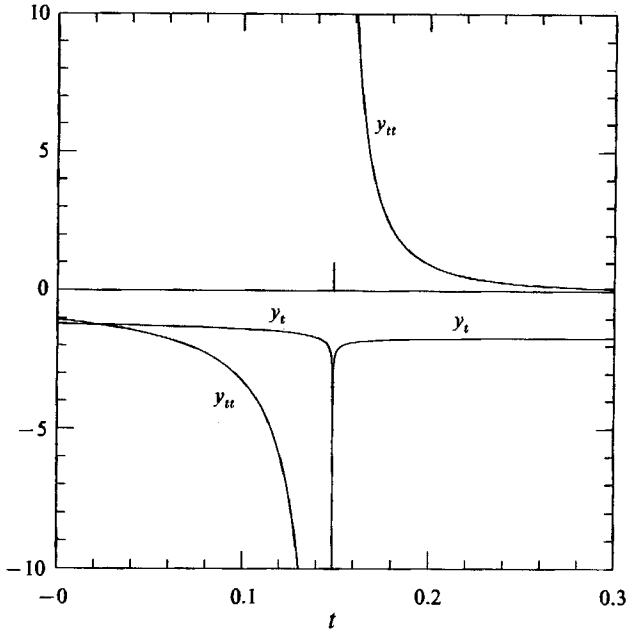

FIGURE 5. The vertical velocity y_t and acceleration y_{tt} of the surface particle $\omega = 0$ in the neighbourhood of $t = t_c$, for the trajectory $(F_0, G_0) = (-1.3, 0)$, $F_0' = 1.0$.

9. Typical solutions, Types A and B

Figure 6 shows a sequence of surface profiles for the Type A trajectory $F_0 = -1.3$. These were obtained by integrating backwards from $t = 0$, when $(F, G) = (F_0, 0)$, $F_0' = 1$, to $t = -5$, and then forwards from $t = 0$ (with the same initial conditions) to about $t = 0.5$.

For large negative values of t we may show that

$$\left.\begin{aligned} F(t) &\sim C_- t + a_0 + a_1 t^{-1} + a_2 t^{-2} + \ldots, \\ G(t) &\sim \alpha + b_1 t^{-1} + b_2 t^{-2} + \ldots, \end{aligned}\right\} \tag{9.1}$$

where a_n and b_n are constants. Thus the gradient of the surface at $\omega = \pm\infty$, namely $G/|F|$, tends to zero like $|t|^{-1}$. When $t = -\infty$ the surface becomes flat.

As t increases from $-\infty$ to about -1 the value of $G/|F|$ increases to a maximum, and the surface develops a hollow, as in figure 6(*a*), with maximum gradient of about 13° when $t = -1$. Then the gradient decreases to zero at $t = 0$, when (F, G) crosses the axis $G = 0$; the hollow 'fills up' and the surface is plane; see figure 6(*b*). The particle velocities, however, do not vanish. The velocity vectors are shown at various points along the surface.

For positive values of t (figure 6*c*) the surface becomes convex, and since $G < 0$ the gradient at infinity is negative. The shock line is crossed at time $t_c = 0.14866$. As shown by the velocity vectors, the velocity undergoes a sharp kick, resulting in an *S*-shaped trajectory for each particle (see figures 6*d* and 12*b*).

As t increases beyond t_c the surface develops a sharp curvature at the crest; see figure 6(*c*). It may be shown that for large positive times t

$$\left.\begin{aligned} F(t) &\sim -\alpha + a_1 t^{-1} + a_2 t^{-2} + \ldots, \\ G(t) &\sim C_+ t + b_0 + b_1 t^{-1} + b_2 t^{-2} + \ldots. \end{aligned}\right\} \tag{9.2}$$

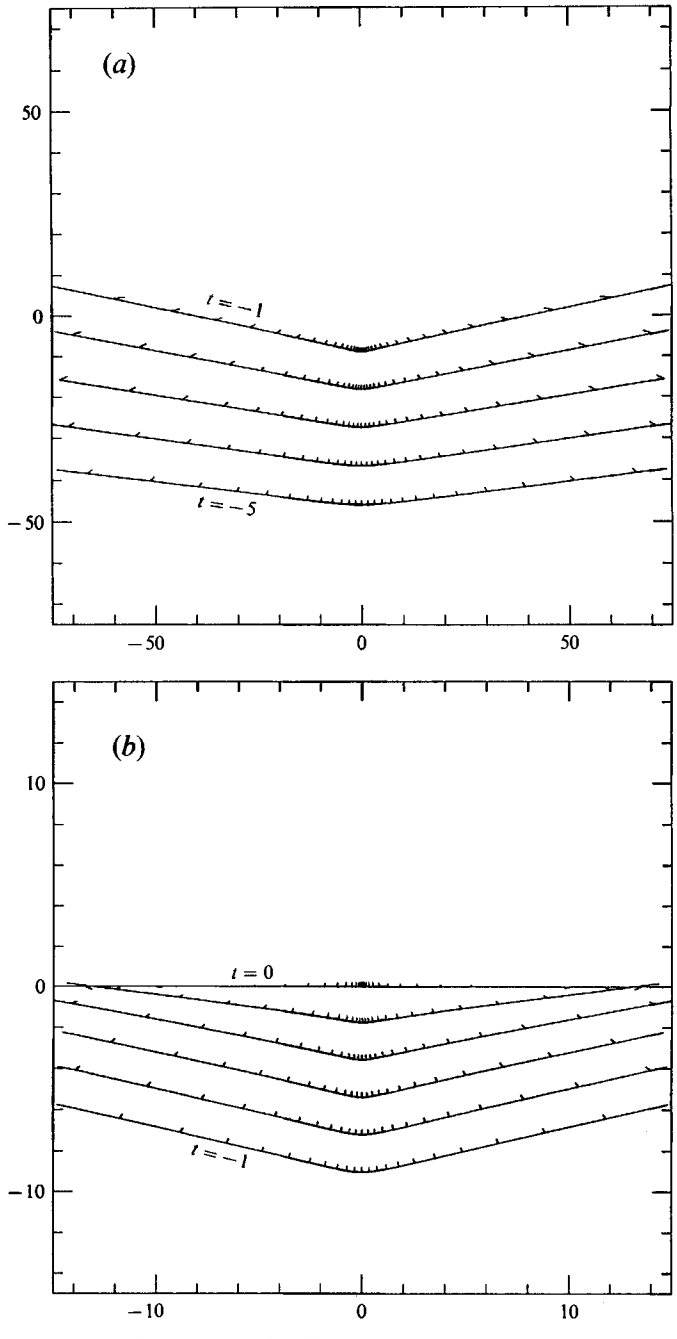

FIGURE 6(a, b). For caption see facing page.

The condition for a cusp, $F = -\alpha$, is not attained in finite time, but only in the limit as $t \to \infty$. Nevertheless the form of the surface is quite close to a cusp even at moderately large times t.

Figure 7 shows a similar sequence of profiles for a typical trajectory of Type B, which does not cross the axis $G = 0$. Thus G is always positive and the surface is always concave. The profiles were obtained by integrating backwards and forwards

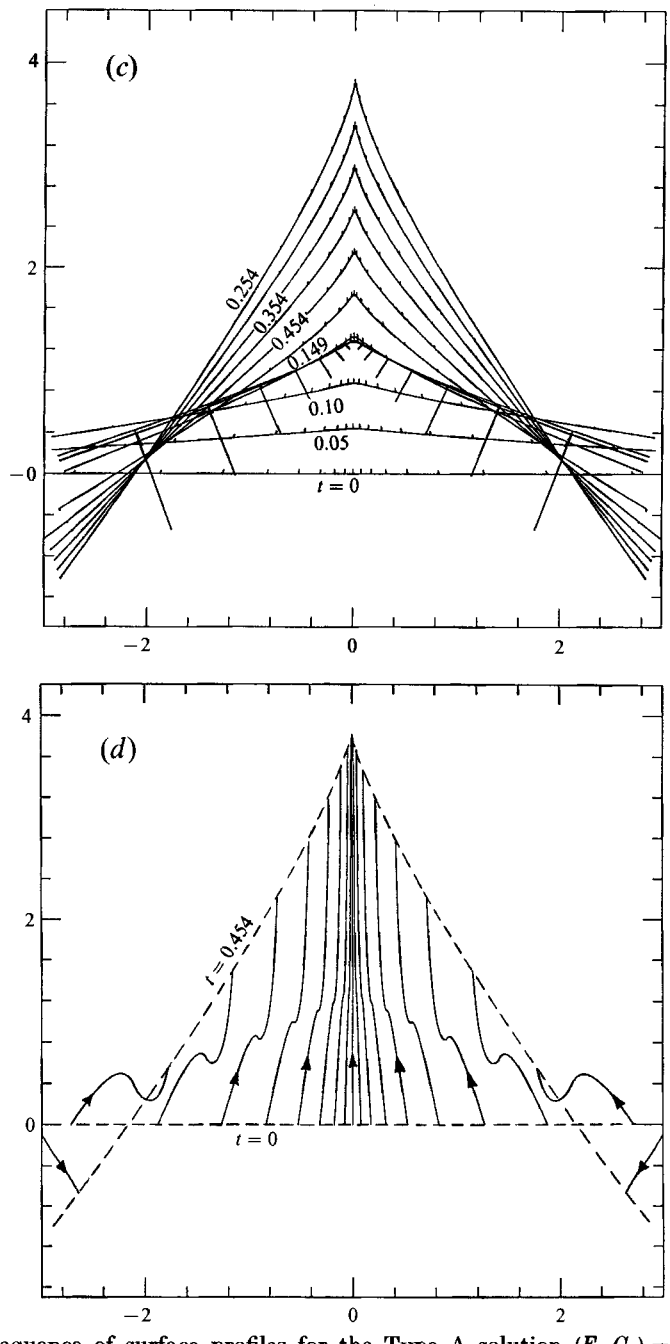

FIGURE 6. A sequence of surface profiles for the Type A solution $(F_0, G_0) = (-1.3, 0)$, $F_0' = 1$, $H_0 = 0$, $H_0' = 10.0$. (*a*) $-5 \leqslant t \leqslant -1$; (*b*) $-1 \leqslant t \leqslant 0$, and (*c*) $0 \leqslant t \leqslant 0.4532$. Velocity vectors are marked for the particles at $\omega = -5.0\ (0.25)\ 5.0$. (*d*) Typical paths of particles in the free surface.

from time $t = 0$ (say) with initial conditions $(F, G) = (-2.0, 0.8)$, $F_0' = 1$. The behaviour as $t \to -\infty$ is similar to that in Type A trajectory; see (9.1). As t increases from $-\infty$ the surface gradient s_∞ at $\omega = \infty$ again increases, so that a hollow develops. The cusp line is always reached in finite time in this type of trajectory but

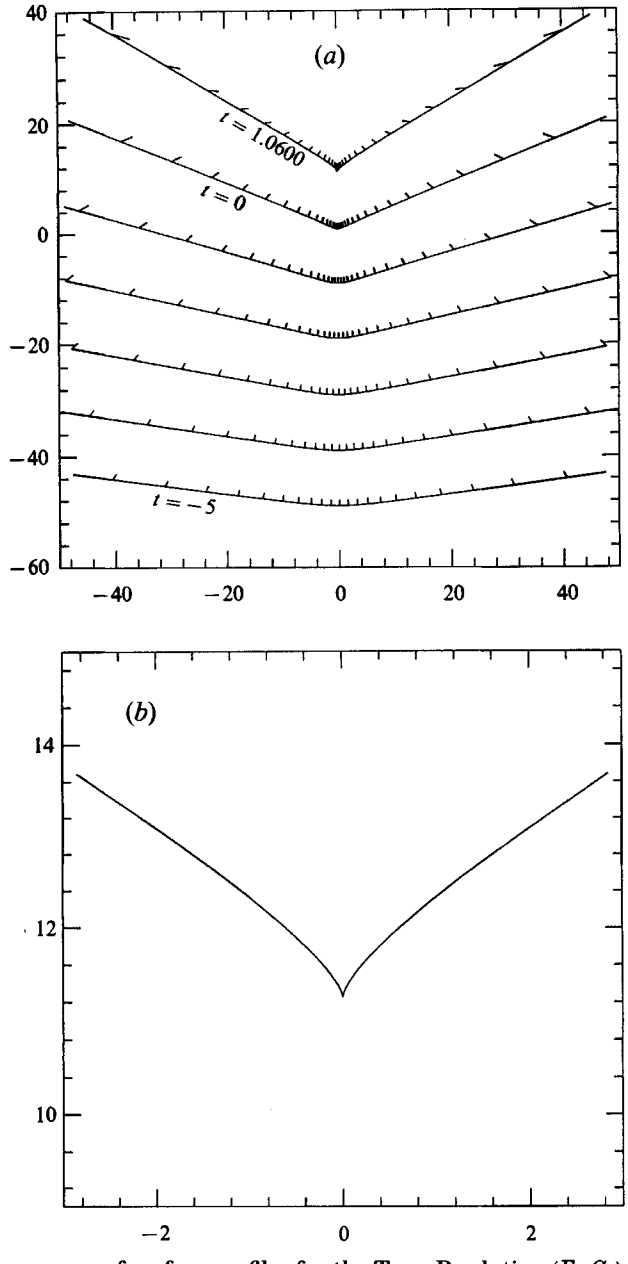

FIGURE 7. (*a*) A sequence of surface profiles for the Type B solution $(F_0, G_0) = (-2.0, 0.8)$, $F_0' = 1$, $H_0 = 0, H_0' = 3.0$, when $-5 \leqslant t \leqslant 1.0600$. (*b*) The downward-pointing cusp in (*a*) at time $t = 1.0600$.

the cusp points downwards. Beyond $F = -\alpha$, the surface profile develops a loop, and the solution becomes unphysical. What happens in practice may be that the sharp cusp entrains some air below the water surface at this point.

The third type of trajectory, which is intermediate between Types A and B will be discussed in the following section.

10. Type C: the critical trajectory

By definition, the critical trajectory is the unique trajectory passing through the point $(F, G) = (-\alpha, 0)$; see figure 3.

To integrate the solution we must first determine the behaviour of $F(t)$ and $G(t)$ near $(-\alpha, 0)$. This point lies on the shock line $(F'G+FG') = 0$, the cusp line $F = -\alpha$ and the critical circle $F^2+G^2 = \alpha^2$. Following the method of §7 by writing

$$F = -\alpha(1+\xi), \quad G = \alpha\eta, \tag{10.1}$$

where now ξ, η are of order ϵ^2 and ϵ respectively, and substituting in (5.1) and setting $\alpha = 1$ we obtain, to lowest order in ϵ,

$$\Phi \equiv -\xi'^2+2\eta\xi'\eta'+2\xi\eta'^2 = 0. \tag{10.2}$$

Now assuming

$$\xi = \tfrac{1}{2}\lambda\eta^2, \quad \xi' = \lambda\eta\eta', \tag{10.3}$$

where λ is a constant to be determined, we have from (10.2) that

$$(-\lambda^2\eta^2+2\lambda\eta^2+\lambda\eta^2)\,\eta'^2 = 0. \tag{10.4}$$

Hence

$$\lambda^2-3\lambda = 0 \tag{10.5}$$

so

$$\lambda = 0 \quad \text{or} \quad 3. \tag{10.6}$$

The solution $\lambda = 0$ applies to the part of the trajectory consisting of the line $F = -\alpha$, $-\infty < G < 0$, and will be considered later. The solution $\lambda = 3$ is the first term in the expansion

$$\xi = \tfrac{3}{2}\eta^2+\tfrac{81}{56}\eta^4+\tfrac{12393}{8624}\eta^6+\ldots, \tag{10.7}$$

which can be used for starting the integration of (F, G) along the part of the trajectory corresponding to $t < 0$.

In addition we have from (4.11) and (7.1)

$$(1+\xi)\,\xi''+\eta\eta'' = 0. \tag{10.8}$$

To lowest order, (10.7) and (10.8) reduce to

$$\xi = \tfrac{3}{2}\eta^2 \tag{10.9}$$

and

$$\xi''+\eta\eta'' = 0 \tag{10.10}$$

respectively. Differentiating (10.9) twice with respect to t and substituting in (10.10) gives

$$4\eta\eta''+3\eta'^2 = 0. \tag{10.11}$$

The general solution of (10.11) tending to 0 as $t \to 0$ is

$$\eta = ct^n \tag{10.12}$$

where

$$4n(n-1)+3n^2 = 0. \tag{10.13}$$

Hence

$$n = \tfrac{4}{7}. \tag{10.14}$$

Thus we have

$$\eta = ct^{\frac{4}{7}}, \quad \xi = \tfrac{3}{2}c^2t^{\frac{8}{7}} \tag{10.15}$$

to lowest order. In addition

$$\left.\begin{aligned} C = 2\xi'\eta'^2 &= \tfrac{384}{343}c^3t^{-\frac{5}{7}}, \\ R = \xi''/\eta &= -\tfrac{12}{49}ct^{-\frac{10}{7}}, \\ \Delta = -C/R &= \tfrac{32}{7}c^2t^{\frac{5}{7}}. \end{aligned}\right\} \tag{10.16}$$

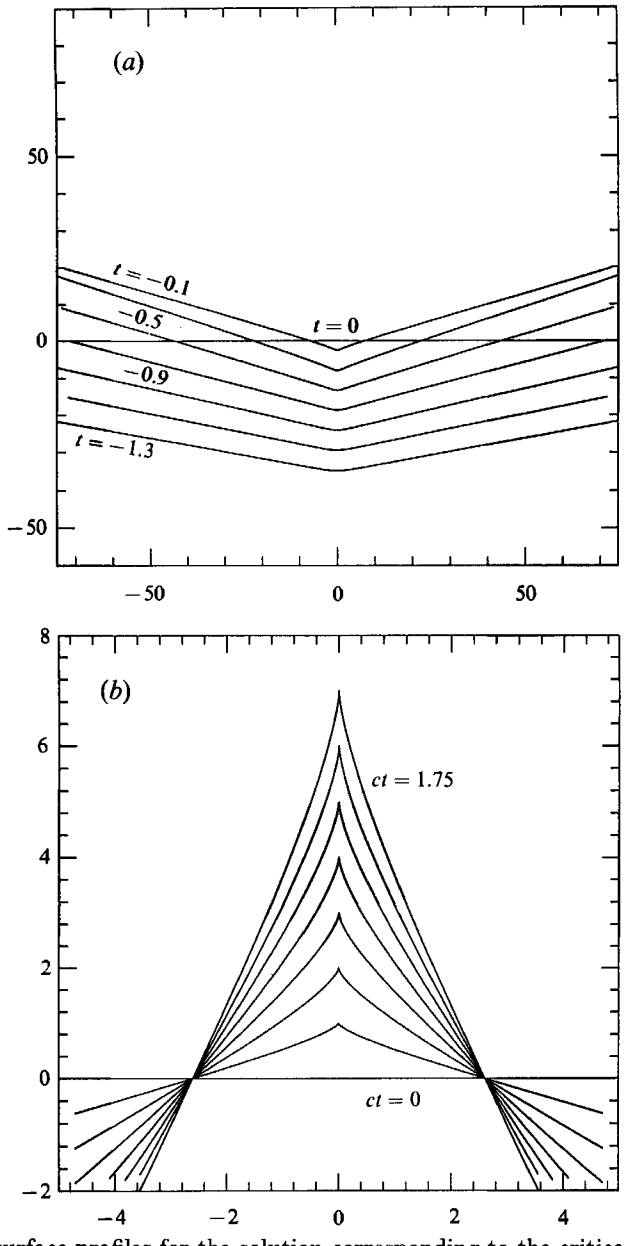

FIGURE 8. The surface profiles for the solution corresponding to the critical trajectory (Type C). (*a*) $t \leqslant 0$, (*b*) $t \geqslant 0$.

Thus the approach to the shock line is still described by a power law, but the powers are different from the general case.

The sequence of surface profiles is shown in figure 8. Again, as $t < -\infty$ the surface is plane. As t increases the surface becomes concave upwards, with a maximum gradient at ∞ given by

$$s_{\max} = (\mathrm{G}/|F'|)_{\max} = \tan 18.6^\circ \tag{10.17}$$

when $t = -0.56$. As $t \to 0$ the surface again reverts to a plane (figure 8*b*), but with a non-zero velocity field. In this case, therefore, it appears that the cusp line is reached in finite time.

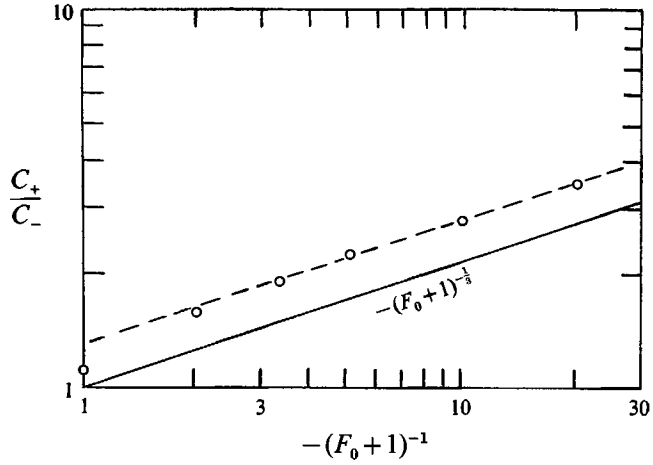

FIGURE 9. The ratio C_+/C_- shown as a function of $-(F_0+1)^{-1}$, when $G_0 = 0$.

F_0	C_-	C_+	C_+/C_-	$-(F_0+1)^{-1}$
$-\infty$	1.0000	−1.0000	−1.000	0.00
−2.0	1.0483	−1.1883	−1.134	1.00
−1.5	1.0996	−1.7218	−1.566	2.00
−1.3	1.1530	−2.1960	−1.905	3.33
−1.2	1.2056	−2.6277	−2.180	5.00
−1.1	1.3102	−3.6451	−2.782	10.00
−1.05	1.4300	−5.0013	−3.497	20.00

TABLE 1. Computed values of C_+/C_- for various values of F_0

For small negative values of t, the solution near the origin is self-similar. In fact by setting $\omega = t^{\frac{4}{7}}\Omega$, $Z = t^{\frac{12}{7}}z$, $c = -\frac{7}{3}$ and choosing a suitable expression for $H(t)$ the surface profile (4.1) reduces to the self-similar form

$$Z \propto \Omega^3 + 7\mathrm{i}\Omega^2 + 49\Omega - \frac{7^3}{15}\mathrm{i} \tag{10.18}$$

studied by Longuet-Higgins (1976).

When $t > 0$, the trajectory of (F, G) continues with uniform velocity down the line $F = -\alpha$, $G < 0$. It is clear that such a solution, with

$$z = \alpha(\omega - \sinh\omega) + \mathrm{i}Vt\cosh\omega + H_0 \tag{10.19}$$

and

$$R \equiv 0 \tag{10.20}$$

is possible with any arbitrary values of the constant velocity V although since $R \equiv 0$ the flow is essentially unaccelerated. The question arises: after passing through the shock line, what should be the appropriate value of V?

This question cannot be answered by direct numerical integration as was done in the general case, because as $F_0 \to -\alpha$ the Taylor expansions about (F_c, G_c) which were previously used have a radius of convergence which tends to zero in the limit. Hence the convergence is non-uniform, and in the limiting case a Taylor expansion is invalid.

However, we may approach the question another way by enquiring what is the ratio of the two constant velocities C_- and C_+ in (9.1) and (9.2). Does the ratio C_+/C_- tend to a finite limit as $F_0 \to -\alpha$?

Table 1 shows the values of C_- and C_+ calculated by numerical time-stepping and extrapolation of $F'(t)$ and $G'(t)$ to $t = -\infty$ and $+\infty$ respectively, for a sequence of values of F_0 approaching $-\alpha$. When plotted logarithmically in figure 9 we see that they follow rather closely a power law; in fact

$$C_+/C_- \sim (F_0+1)^{-\frac{1}{3}} \tag{10.21}$$

approximately. We conclude that the upwards velocity of the crest of the surface profile should be considered as infinite, in the limiting case. In figure 8(*b*) we show the surface profiles developing in time, but scaled by this infinite velocity. Apart from the scaling factor, the solution is quite similar to the finite solution shown in figure 6(*c*), beyond about $t = 0.2$.

11. The general case $\beta \neq 0$

From §5 onwards we have assumed that $\beta = 0$. We come now to the general case $\beta \neq 0$.

In the first place, since $\gamma = \alpha+\beta t$, we can change the origin of the time t so as to make $\alpha = 0$. Thus

$$\gamma = \beta\tilde{t} \quad \text{where} \quad \tilde{t} = t+\alpha/\beta. \tag{11.1}$$

We shall assume this done, and then suppress the tilde.

From (4.10) the expression for Φ becomes simply

$$\Phi \equiv (F'G+FG')^2-\beta^2[(F-tF')^2+(G+tG')^2]. \tag{11.2}$$

To simplify the factor multiplying β^2 we set

$$F = tP(t), \quad G = t^{-1}Q(t) \tag{11.3}$$

giving

$$(P'Q+PQ')^2-\beta^2(t^4P'^2+Q'^2) = 0, \tag{11.4}$$

which can be written

$$(Q^2-\beta^2t^4)P'^2+2PQP'Q'+(P^2-\beta^2)Q'^2 = 0. \tag{11.5}$$

Provided that

$$D \equiv P^2+Q^2/t^4-\beta^2 > 0 \tag{11.6}$$

(11.5) defines two characteristic directions in the (P, Q)-plane given by

$$\frac{P'}{Q'} = \frac{1}{t^2}\frac{(-PQ/t^2 \pm \beta t^2 D^{\frac{1}{2}})}{Q^2/t^4-\beta^2}. \tag{11.7}$$

As before, if $\beta > 0$, a choice of the positive sign in (11.7) annuls the branch point which lies below the free surface. The condition (11.6) implies now that (P, Q) must lie outside the ellipse

$$P^2+Q^2/t^2 = \beta^2, \tag{11.8}$$

having semi-axes β and βt respectively. This ellipses touches the cusp line, which is given by $P = -\beta$.

The time-dependence can be found by differentiating (11.2) with respect to t as before. Substituting for the second derivatives F'' and G'' from (4.5) we then get

$$R = C/A \tag{11.9}$$

where now

$$\left.\begin{aligned} C &= (F'G+FG')\,2F'G'-\beta^2(G+tG')\,G', \\ A &= (F'G+FG')\,(F^2-G^2)-\beta^2t[(F'-tF)\,G+tFG']. \end{aligned}\right\} \tag{11.10}$$

In terms of P and Q, A can be expressed as

$$A/t^2 = (P'Q+PQ')\,(P^2-Q^2/t^4)+\beta^2(P'Q-PQ'). \tag{11.11}$$

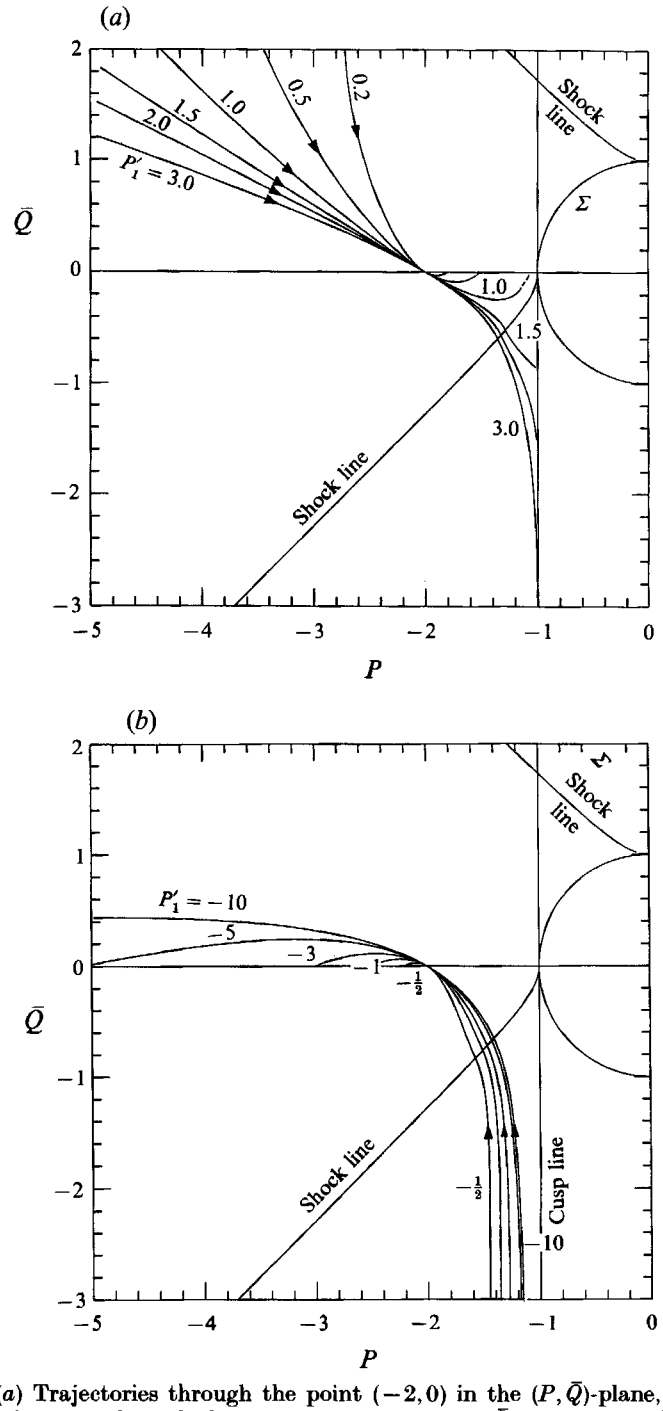

FIGURE 10. (*a*) Trajectories through the point $(-2, 0)$ in the $(P, \bar{Q})$-plane, when P_1' is positive. (*b*) Trajectories through the point $(-2, 0)$ in the $(P, \bar{Q})$-plane, when P_1' is negative.

Now substituting for β^2 from (11.4) we obtain

$$\frac{\Delta}{t^2} = \frac{(PQ'+P'Q)(PP'+QQ'/t^4)(PP'-QQ'/t^4)}{P'^2+Q'^2/t^4}. \tag{11.12}$$

The factor $(PP'-QQ'/t^4)$ can be shown to vanish only on the ellipse (11.3), and the shock line is given by

$$(PP'+QQ'/t^4) = 0. \tag{11.13}$$

Now (11.13) can be written

$$\frac{t^2P'}{Q'} = -\frac{Q/t^2}{P}. \tag{11.14}$$

Since t^2P'/Q' is also given by (11.7), we see that the equation of the cusp locus is a function only of P and Q/t^2, independently of other variables. And it is the same equation as in the case $\beta = 0$ treated earlier, except that now P, Q/t^2 and β take the place of F, G and α.

Suppose then that we set

$$\bar{Q} = Q/t^2. \tag{11.15}$$

Then in the $(P, \bar{Q})$-plane, but not in the (P, Q)-plane or the (F, G)-plane, the equation of the shock line is invariant with respect to the time. So also is the boundary (11.8), which becomes the 'circle'

$$P^2+\bar{Q}^2 = \beta^2, \tag{11.16}$$

and also the cusp line, $P = -\beta$. It is clearly advantageous, therefore, to map the trajectories of (F, G) in the $(P, \bar{Q})$-plane, where these crucial features stay put (see figure 10), rather than in either of the other two planes.

12. Typical solutions: $\beta \neq 0$

Consider the initial conditions. Unlike the case $\beta = 0$, the origin of time has now been fixed. Moreover in (11.2), β defines the scale of the velocities. The solutions to (11.2) and (4.13) have arbitrary lengthscale, but this is related to their timescale by the chosen velocity β.

We may assume $\beta > 0$. For the solution to be valid below the free surface, βt must be positive, hence $t > 0$. As a 'typical' instant let us take $t = 1$. The value of $(P, \bar{Q})$ at time $t = 1$ then determines the lengthscale of motion. The velocity scale may be determined by choice of P' (or F') at time $t = 1$. The value of Q' (or G') is then determined by (11.2). Thus through any given point $(P_1, \bar{Q}_1)$, at a given time $t = 1$, there is a singly infinite family of solutions, with parameter P'_1, say.

To fix the ideas let us take $(P_1, \bar{Q}_1)$ on the negative $\bar{Q}$-axis, so $\bar{Q}_1 = 0$. This has the advantage that the gradient $(P'_1, \bar{Q}'_1)$ at the initial point is fixed; for then

$$Q' = (t^2\bar{Q})' = t^2\bar{Q}' + 2t\bar{Q} = t^2\bar{Q}' \tag{12.1}$$

and so by (11.7)

$$P'/\bar{Q}' = \pm(P^2/\beta^2-1)^{\frac{1}{2}} \tag{12.2}$$

independently of the initial value of P'. Therefore the trajectories passing through such a point touch either of two fixed lines. These lines are the two tangents from $(P_1, 0)$ to the critical circle Σ; see figure 10.

Figure 10 shows the family of trajectories of $(P, \bar{Q})$ passing through the typical point $(P_1, \bar{Q}_1) = (-2, 0)$ on the $\bar{Q}$-axis. When $P'_1 > 0$ (figure 10*a*) each of the trajectories tends to an asymptote going to infinity in the upper left-hand quadrant, as $t \to 0$. The coefficients F and G then tend to constant, non-zero values. On the other hand if $t \to +\infty$, then so long as $P'_1 > P'_{1\text{crit}} \approx 1.087$, each trajectory tends to a limit

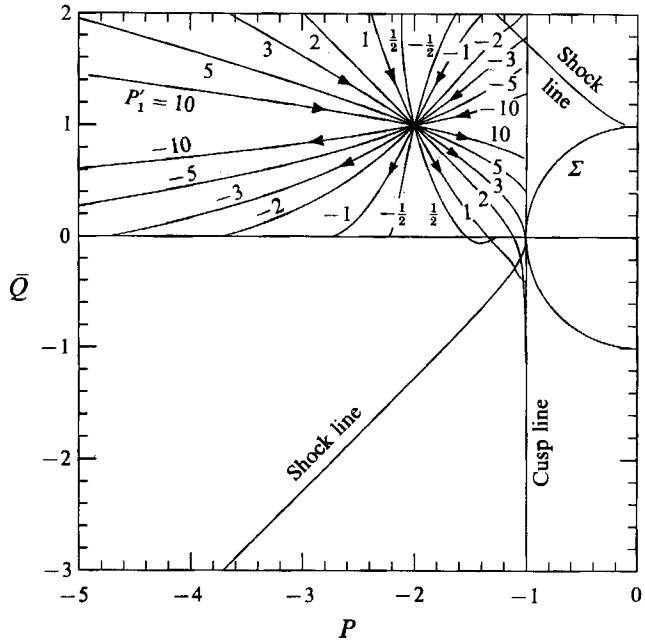

FIGURE 11. Trajectories through the point $(-2, 1)$ in the $(P, \bar{Q})$-plane.

point $(-\beta, \bar{Q})$ on the cusp line ($P = -\beta$). Each trajectory also crosses the shock line at some instant $t = t_c$, where P and $\bar{Q}$ behave like $(t-t_c)^{\frac{2}{3}}$, as described in §7. Since the limit points of P and Q are not at the origin, F and G must behave asymptotically like t. The free surface is then of the form

$$z \sim t(L \sinh \omega + iM \cosh \omega - \beta\omega), \tag{12.3}$$

where L and M are constants. This is a cusped curve of fixed shape, with dimensions increasing linearly with time.

However, when $0 < P_1' < P_{1\,\mathrm{crit}}'$ the trajectories do not cross the shock line, but instead tend to limit points on the $\bar{Q}$-axis. In the critical case $P_1' = P_{1\,\mathrm{crit}}'$ the trajectory touches the shock line.

The asymptotic behaviour of F and G at the limit points can be investigated by writing

$$F = t(\lambda + \xi), \qquad G = t(\mu + \eta), \tag{12.4}$$

where λ and μ are constants and ξ, η tend to 0 in the limit. On substituting in (11.2) we find to lowest order

$$\Phi \equiv 4(\lambda^2 - \beta^2)\mu^2 t^2, \tag{12.5}$$

which must vanish for all values of t. Hence either $\lambda = -\beta$ or $\mu = 0$. The first case describes the limit points on the cusp line. The second case describes the limit points on the $\bar{Q}$-axis.

For sufficiently small values of P_1', the asymptote to the trajectory as $t \to 0$ makes an angle greater than 45° with the negative $\bar{Q}$-axis. Hence the trajectory must intersect the second shock line, touching the circle Σ at the point $(0, \beta)$; see figure 10(*a*).

On the other hand, when $P_1' < 0$ (figure 10*b*), each trajectory has an asymptote $P = P_0$ as $t \to 0$. It then crosses the shock line and as $t \to \infty$ tends to a limit point on the negative $\bar{Q}$-axis. The free surface is asymptotically flat.

Figure 11 shows the family of trajectories through a point (P_1, Q_1) lying *off* the $\bar{Q}$-axis. The family contains some curves which cross the cusp line above the point

$(-\beta, 0)$. In these, the free surface develops downward-pointing cusps at a finite time t, which subsequently develop into loops. There exists a family of such trajectories passing through the point $(-\beta, 0)$. The limiting form of the free surface is derived below in Appendix B.

13. Discussion and conclusions

We have found and described a class of simple, time-dependent solutions of the non-linear equations for potential flow with a free surface which are of special interest for two reasons: (*a*) the free surface can form a cusp, in finite or infinite time, and (*b*) the flow develops an inertial shock (not related to the formation of the cusp) through which it can pass and continue on the other side. At the shock itself the fluid velocity, pressure and acceleration become momentarily infinite, but the displacements are bounded.

The solutions described in this paper satisfy the boundary conditions for time-dependent, irrotational flow exactly. Both gravity and surface tension have of course been neglected. This means that the solutions apply strictly only to those parts of the flow where the acceleration greatly exceeds g. The role of gravity is simply to help set up the initial conditions under which an inertial shock can develop. Since gravity and surface tension are always present, the solutions described here must be regarded as asymptotic forms to which the actual flow will tend, as is suggested by the experiments noted in §1. However, the range of initial conditions which ultimately give rise to a flow having this asymptotic form, though a very interesting problem, is beyond the scope of this paper.

It is natural to ask whether the occurrence of an 'inertial shock' is in any way related to the formation of a cusp at the free surface. However, by considering the special case of the Dirichlet hyperbola which displays shock behaviour (see Appendix A) but no cusp, it will be apparent that the two phenomena are not closely related. The Dirichlet hyperbola is, moreover, an exact solution, with no weak discontinuities in the interior of the fluid such as occur in the general case (see §5).

Do these weak discontinuities completely negate the interest of these flows in the general case? In our opinion they do not; because the discontinuities are only weak, in a certain sense, it may be possible to treat each solution as the first in a series of approximations to a more exact solution.

The present model is the beginning to a more extensive study of this hitherto unrecognized phenomenon. In future work, the theory will be developed in several different directions:

(i) Analogous solutions in which circular functions of ω take the place of hyperbolic functions in the expression for $z(\omega, t)$. These describe motions that are periodic (wave-like) in the x-direction, though not necessarily in time (see Longuet-Higgins 1993*a*).

(ii) By adding to the right-hand side of (4.1) two further terms in $\sinh 2\omega$ and $\cosh 2\omega$ respectively one obtains a class of time-dependent solutions in which the pressure and acceleration attain very large values near a critical instant, but nevertheless remain finite (Longuet-Higgins 1993*b*). This dismisses any doubts as to the physical significance of the model.

(iii) By allowing the coefficients $F(t)$ and $G(t)$ to become complex instead of real, one can obtain solutions with a sense of rotation, as was previously done for the Dirichlet hyperbola (Longuet-Higgins 1983*a*, *b*). These solutions may be applicable to breaking waves, particularly plunging breakers, which sometimes develop high accelerations.

(iv) There is reason to suspect the existence of analogous axisymmetric solutions, in parametric form, which will describe the well-known occurrence of inertial jets in collapsing bubbles.

This work has been supported by the Office of Naval Research under Grant No. N00014-91-J-1582.

Appendix A. Particle paths in a Dirichlet hyperbola

Equations (3.5) and (3.11) admit an exact analytic solution as follows. Let us write

$$B = F/F' = -G/G' \tag{A 1}$$

so that
$$F = \exp\left(\int \frac{1}{B}\,\mathrm{d}t\right), \quad G = -\exp\left(\int \frac{-1}{B}\,\mathrm{d}t\right), \tag{A 2}$$

where we have chosen the unit of length so that the constant on the right of (3.11) equals -1. Then on differentiating (A 1) we have

$$(1-B')F'^2 + (1+B')G'^2 = FF'' + GG'' = 0 \tag{A 3}$$

by (3.5). Hence
$$(B'-1)F^2 = (B'+1)G^2, \tag{A 4}$$

and on differentiating each side logarithmically we get

$$\frac{B''}{B'-1} + \frac{2}{B} = \frac{B''}{B'+1} - \frac{2}{B}, \tag{A 5}$$

hence
$$BB'' + 2B'^2 = 2. \tag{A 6}$$

A first integration yields

$$B^4B'^2 - B^4 = \text{constant} = 1, \tag{A 7}$$

say, by choice of the unit of time. Therefore

$$B'^2 = (1+B^4)/B^4 \tag{A 8}$$

and so
$$t = \pm \int \frac{B^2}{(1+B^4)^{\frac{1}{2}}}\,\mathrm{d}B. \tag{A 9}$$

We may choose the origin of time at $B = 0$. It follows from (A 2) that

$$F = \exp\left[\pm \int \frac{B}{(1+B^4)^{\frac{1}{2}}}\,\mathrm{d}B\right] \tag{A 10}$$

and that $G = -1/F$. The path of a particle at the free surface (ω fixed and real) relative to a frame moving downwards with speed V is now given parametrically by

$$x = F\sinh\omega, \quad y = Vt - F^{-1}\cosh\omega. \tag{A 11}$$

When $B \ll 1$ we have from (A 9) that $t \sim \frac{1}{3}B^3$, so $B \sim (3t)^{\frac{1}{3}}$ and so from (A 10)

$$F \sim 1 \pm \tfrac{1}{2}(3t)^{\frac{2}{3}}. \tag{A 12}$$

Thus the particle velocity becomes infinite like $t^{-\frac{1}{3}}$ and there is a typical weak 'shock'.

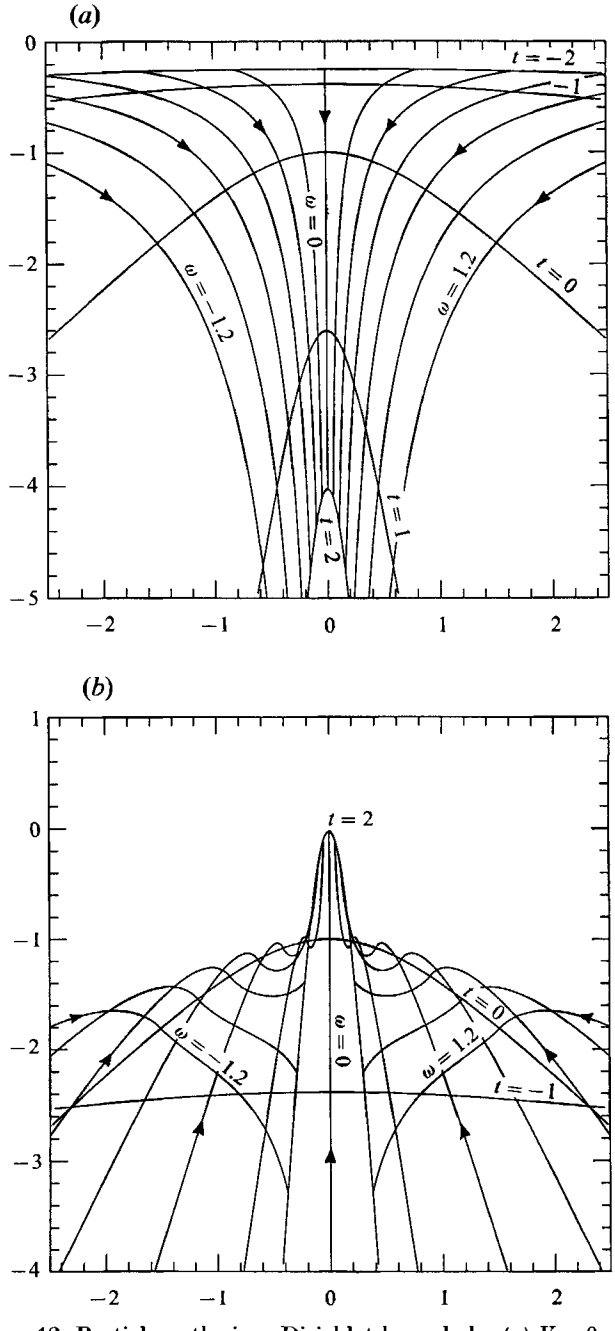

FIGURE 12. Particle paths in a Dirichlet hyperbola. (*a*) $V = 0$; (*b*) $V = 2$.

In the special case $V = 0$, the particle paths satisfy $xy =$ constant and all are hyperbolae; see figure 12(*a*). The large velocities near $t = 0$ are not immediately obvious. However, if we view the trajectories in a moving reference frame by taking $V = 2$, for example, we get figure 12(*b*), in which the typical S-shaped kinks appear.

This shows that the kinks are in a sense artifacts of the reference frame. On the other hand they could be useful experimentally as a diagnostic for weak shocks.

Appendix B. The limiting form of trajectories through the point $(-\beta, 0)$ as $t \to \infty$

For large values of the time t, the coefficients F and G have the asymptotic expansions

$$F = -\beta t(1 + a_1 t^{2\nu} + a_2 t^{4\nu} + \ldots), \quad G = \beta t(b_1 t^{\nu} + b_2 t^{3\nu} + \ldots). \tag{B 1}$$

where ν is a negative index. Substituting into (11.2) and (4.11) we find to lowest order

$$\Phi \equiv [2(\nu+2)(3\nu+2)\, a_1 b_1^2 - (2\nu)^2 a_1^2]\, t^{4\nu+2} = 0 \tag{B 2}$$

and

$$FF'' + GG'' \equiv [2\nu(2\nu+1)\, a_1 + \nu(\nu+1)\, b_1^2]\, t^{2\nu} = 0 \tag{B 3}$$

respectively. On eliminating the ratio a_1/b_1^2 from these equations we obtain a cubic equation:

$$7\nu^3 + 20\nu^2 + 16\nu + 4 = 0 \tag{B 4}$$

for the exponent ν, which has only one real solution, namely

$$\nu = -1.7231. \tag{B 5}$$

Correspondingly we find

$$a_1/b_1^2 = -0.1478. \tag{B 6}$$

When $\omega/t^{\nu} \ll 1$ it is easily shown that the free surface has the self-similar form

$$Z = \Omega^3 - \frac{3\mathrm{i}}{\nu+1}\Omega^2 - \frac{3}{(\nu+1)(2\nu+1)}\Omega + \frac{\mathrm{i}}{(\nu+1)(2\nu+1)(3\nu+1)} \tag{B 7}$$

in which

$$\Omega = \frac{(\nu+1)}{b_1^3}\frac{\omega}{t^{\nu}} \quad \text{and} \quad z = \frac{-6}{(\nu+1)^3}\frac{z}{t^{3\nu+1}}, \tag{B 8}$$

(see Longuet-Higgins 1976, §9).

REFERENCES

Cooker, M. J. & Peregrine, D. H. 1990 Violent water motion at breaking-wave impact. In *Coastal Engineering (Proc. ICCE Conf., Delft, Holland)*, vol. 1, pp. 164–176. ASCE.

John, F. 1953 Two-dimensional potential flows with a free boundary. *Commun. Pure Appl. Maths* **6**, 497–503.

Longuet-Higgins, M. S. 1972 A class of exact, time-dependent, free-surface flows. *J. Fluid Mech.* **55**, 529–543.

Longuet-Higgins, M. S. 1976 Self-similar, time-dependent flows with a free surface. *J. Fluid Mech.* **73**, 603–620.

Longuet-Higgins, M. S. 1983*a* On the forming of sharp corners at a free surface. *Proc. R. Soc. Lond.* A **371**, 453–478.

Longuet-Higgins, M. S. 1983*b* Towards the analytic description of overturning waves. In *Nonlinear Waves* (ed. L. Debnath), pp. 1–24. Cambridge University Press, 360 pp.

Longuet-Higgins, M. S. 1983*c* Bubbles, breaking waves and hyperbolic jets at a free surface. *J. Fluid Mech.* **127**, 103–121.

Longuet-Higgins, M. S. 1993*a* Highly-accelerated, free-surface flows II. Space-periodic solutions. (To be submitted.)

Longuet-Higgins, M. S. 1993*b* Highly-accelerated, free-surface flows. III. Inertial shocks of bounded intensity. (To be submitted.)

Nishimura, H. & Takewaka, S. 1990 Experimental and numerical study on solitary wave breaking. In *Coastal Engineering (Proc. ICCE Conf., Delft, Holland)*, vol. 1, pp. 1033–1045. ASCE.

Peregrine, D. H. & Cooker, M. J. 1991 Violent motion as near-breaking waves meet a wall. *Proc. IUTAM Symp. on Breaking Waves, Sydney, Australia, July 1991.*